

Shen-Qi-Wan Protects the Renal Peritubular Capillary From Adenine-mediated Damage by Upregulating Aquaporin 1

Yuting Bao

Zhejiang Chinese Medical University

Yehui Zhang

Zhejiang Chinese Medical University

Yuanxiao Yang

Hangzhou Medical College

Xueming Chen

Zhejiang Chinese Medical University

Luning Lin

Zhejiang Chinese Medical University

Yunbo Fu

Zhejiang Chinese Medical University

Liting Ji

Zhejiang Chinese Medical University

Changyu Li (✉ lcyzcmu@sina.com)

Department of pharmacology, University of Zhejiang Chinese Medical, Hangzhou 310006, Zhejiang, China <https://orcid.org/0000-0001-8656-0428>

Research

Keywords: Chronic kidney disease, Peritubular capillary injury, Shen-Qi-Wan, AQP1, VEGF

Posted Date: November 18th, 2020

DOI: <https://doi.org/10.21203/rs.3.rs-107303/v1>

License: © ⓘ This work is licensed under a Creative Commons Attribution 4.0 International License.

[Read Full License](#)

Abstract

Background Shen-Qi-Wan (SQW), a commonly used prescription against chronic kidney disease (CKD) in Traditional Chinese Medicine (TCM), has a nephroprotective action in adenine-induced kidney injury. However, the mechanism of SQW in renal injury remains unclear.

Methods: We evaluated the nephroprotective action of SQW in adenine-induced kidney injury and investigated its mechanism in vitro studies.

Results: SQW supplementation could alleviate the pathological makers for CKD, ameliorate dysfunction of Hypothalamic-Pituitary-Adrenal (HPA) axis and renal function loss caused by adenine. Alternatively, SQW administration showed an ameliorating effect from the toxicity and alleviated the injury of capillaries around renal tubules instigated by adenine through increasing AQP1 mRNA and protein level. In vitro experiments, SQW medicated serum enhanced the migration and lumen formation ability of HMEC-1 cells, and significantly increased AQP1 protein level. Moreover, AQP1 knockdown efficiently inhibited migration and lumen formation ability in HMEC-1 cells which could be reversed by SQW medicated serum.

Trial registration : This is an animal and cell experiment, trial registration is not necessary.

Conclusion: These results suggested that SQW attenuated peritubular capillary injury in adenine induced CKD model rats through boosting angiogenesis in endothelial cell and AQP1 may be a potential target of SQW for treating renal injury.

Introduction

Chronic kidney disease (CKD), also called chronic kidney failure, describes the gradual loss of kidney function due to different issues like- type- 1 or 2 diabetes, high blood pressure, glomerulonephritis, interstitial nephritis, polycystic kidney disease. In other cases, prolonged obstruction of the urinary tract, from conditions such as enlarged prostate, kidney stones, and some cancers can also form CKD (1). CKD formation can be of a short or long period due to the functional damages of the kidney. It is considered a severe public health problem that leads to death, due to the failure in the cardiovascular system and renal system (2). It was estimated that about 10% of the world population afflicted with CKD (3). Therefore, in this article, we examined the prevention and therapy measures for CKD in a preclinical system.

The pathological syndrome of CKD includes glomerular sclerosis (4), tubular atrophy (5), and interstitial fibrosis (6). Another cause for the decreased renal function is peritubular capillary injury, a major risk factor for CKD (7). There is a probability to withstand with the CKD is to targeted repair of peritubular capillary endothelium (8, 9). The endothelial cells (ECs) could be used to regenerate the new blood vessels via angiogenesis and thus far these cells are known to involve in cell migration and proliferation. Moreover, repairing the renal layers can restore the oxygen supply to renal tubules and the delivery of nutrients (10). Improvement in understanding the relation between endothelium and CKD can open up the

horizon for novel therapies. Therefore, in this article, we considered examining the relationship of the angiogenesis endothelial cell and renal tubule injury.

The nontoxic medicines are rare in the present scenario; the alternative herbal medicines could be a remedy due to their antioxidant nature. Traditional Chinese medicines have plenty of beneficiary property, but lack of scientific pieces of evidence prevents them from use as mainstream. Therefore, in this article, we examined the beneficiary property of one popular Chinese herbal on CKD. Shen Qi Wan (also known as Gui Fu Di Huang Wan; SQW) is a famous Chinese alternative medicine cocktail recipe, traditionally used as a kidney disorder. SQW tend to be overprescribed in modern Chinese herbalism (chronic exhaustion disorders in contemporary patients tend to primarily involve Spleen and Liver imbalances), the remedy constitutes one of the fundamental paths for addressing chronic kidney issues and thus covers a wide range of pathologies. The classic recipes of SQW were first recorded in Zhang Zhongjing's *Jingui Yaolue* and traditionally used in the clinical treatment of CKD (11). The components of SQW are made up of eight Chinese traditional herbs which are listed in Table 1. In a recent study, SQW treatment was alleviated renal morphological changes, and reduced inflammatory activity, glomerular necrosis in adenine induced CKD model rats (12). Studies demonstrated that components that consist of SQW are closely associated with the angiogenesis process. Diosgenin (extracted from the root of wild yam) treatment enhanced endothelial proliferation and angiogenesis via activating HIF-1 α and VEGF pathway thus helps in boosting bone formation and fracture healing (13). Catalpol, an active component of *Radix Rehmanniae*, used in the treatment of neurodegenerative diseases, ischemic stroke, metabolic disorders. Moreover, experiments showed that catalpol can improve angiogenesis in rats' stroke model (14). However, the mechanism of SQW in boosting angiogenesis was rarely investigated.

Table 1
Eight herbal medicines in Shen-Qi-Wan

Chinese names	Pharmacognostic nomenclature	Botanical nomenclature	Proportion of ingredients(100%)
Dihuang	Rehmanniae Radix Praeparata	<i>Rehmannia glutinosa</i> Libosch.	29.7%
Danpi	Moutan Cortex	<i>Paeonia suffruticosa</i> Andr.	11.1%
Shan Zhuyu	Corni Fructus	<i>Cornus officinalis</i> Sieb. et Zucc.	14.8%
Fulin	Poria	<i>Poria cocos</i> (Schw.) Wolf	11.1%
Shanyao	Dioscoreae Rhizoma	<i>Dioscorea opposita</i> Thunb.	14.8%
Zhexie	Alismatis Rhizoma	<i>Alisma orientalis</i> (Sam.) Juzep.	11.1%
Rougui	Cinnamomi Cortex	<i>Cinnamomum cassia</i> Presl	3.7%
Fuzi	Aconiti Lateralis Radix Praeparata	<i>Aconitum carmichaelii</i> Debx.	3.7%

Aquaporin (AQPs) membrane receptors are extremely abundant in the nephron. AQPs act as membrane water channels that involve in secretion and absorption of water and maintain the osmotic balance of the cell membrane (15). The majority of AQP1 is distributed in the proximal and basement membrane cells of the proximal tubules of the kidney, the descending branch of medullary stenosis and the small vascular endothelial cells (16). To overcome CKD microvascular repair and angiogenesis in renal tubular involves mitigating the damage (17). Moreover, increasing evidence disclosed that AQP1 involves the microvessel formation and cell migration (18, 19), thus, AQP1 facilitated endothelial cell angiogenesis that could ameliorate renal dysfunction. Based on the above research background, we hypothesized that SQW treatment may promote angiogenesis in the endothelial cell that can reduce renal injury. We used adenine induced peritubular capillary injury in the kidney in the rat model system. We examined the beneficiary effect of SQW on our induced CKD model system also explored whether SQW was able to improve the perivascular circumference by boosting angiogenesis in AQP1 knockdown-HMEC-1.

Materials And Methods

2.1. Drugs

SQW, Chinese patent medicine, was purchased from Henan Wanxi Pharmaceutical Co., Ltd.(Henan, China). Its batch number is 161101. The quality control of SQW of different batch number measured by high performance liquid chromatography (HPLC) analysis achieved the requirements of the 2015 version

of Chinese Pharmacopoeia (20). The total average quantity of morroniside and loganin was 6.46 mg/g and the average content of paeonol was 4.3 mg/g. We also detected the main five components (higenamine, coryneine chloride, salsolinol, o-anisaldehyde, and cinnamic acid) which belong to the *jun* herbs *Ramulus Cinnamomi* and *Radix aconiti lateralis preparata* by Ultra-Performance Liquid Chromatography (UPLC) (21).

2.2. Animals

The animal experiment was approved by the Ethics of Committee of Zhejiang Traditional Chinese Medical University (Laboratory breeding room license number: SYXK (Zhejiang) 2013 – 0184). Male SD rats in SPF grade (age 8 weeks; weight 250 ± 10 g) were purchased from Shanghai Xipuer Bikai Experimental Animal Co. Ltd. (Laboratory animal production license number: SCXK (Shanghai) 2013-0016. Ethical review resolution number: ZSLL-2017-054). The rats were housed in ambient optimal temperature ($20 \pm 2^\circ\text{C}$) and humidity and sterilized food and water were provided. *All 30 rats were randomly divided into control group (n = 6) and model group (n = 24). In order to establish kidney yang deficiency model, the rats in model group were administrated with adenine (150 mg/kg/d) by intra-gastric way for constant 14 days. Then 24 model rats were randomly divided into model group (n = 6) and three doses of SQW group (1.5 g/kg/d, 3 g/kg/d, and 6 g/kg/d; n = 6 in each sub-groups). The model group was continuously administrated with 150 mg/kg adenine for 3 weeks. Meanwhile, three doses of SQW groups were co-administrated with SQW of different doses and adenine (150 mg/kg/d) for 21 days. The saline was used for the control group. The volume of gavage was 0.1 ml/10 g. The clinical equivalent dose of SQW was calculated according to the conversion method of the dosage of experimental animals and humans (calculated by the ratio of the body surface area of 200 g rats with standard weight and 70 kg humans). According to the clinical dosage of this formula, the dosage of 3.0 g/kg SQW is equivalent to 3 times the clinical dosage.*

2.3. H&E Staining

The kidney tissues from each group were fixed in 10% formaldehyde. After paraffin embedding, the tissues were sectioned into 3–5 μm thickness for H&E staining. The pathological conditions of renal tissues from different groups were observed under a light microscope (Leica, Germany). The results of H&E staining were used to observe the morphology and structure of the rat's kidney tissue under an optical microscope.

2.4. ELISA

After completing the treatment tenure, the hypothalamus, serum and urine samples were collected. With the isolated hypothalamus 9 volumes of PBS (Solarbio, Beijing, China) were added and centrifuged at 2000 rpm for 10 min. Collected blood samples were centrifuged at 3000 rpm for 10 min. The urine was collected and centrifuged at 3000 rpm for 5 min. The level of ACTH, CORT, VCAM-1, VEGF and 24 UTP were measured according to the manufacturer's instructions in the ELISA kit (Shanghai Xinfan Biotechnology, Shanghai, China). The automatic biochemical detector is used to detect the content of blood urea nitrogen (BUN), serum creatinine (Scr) and urinary 17-hydroxy corticosteroid (17-OHCS).

2.5. Immunohistochemistry

Paraffin-embedded renal sections (3–5 μm) were baked in an incubator at 60 °C for 2 h and then washed in distilled water for 2 min. The tissue sections were quenched using 3% H_2O_2 for 10 min and then washed in PBS. Tissue sections were then incubated with anti-Aquaporin 1 primary antibody (Abcam, Cambridge, UK), anti-CD34 primary antibody (HUABIO, Hangzhou, China) and anti-VEGF primary antibody (HUABIO, China) at 37 °C for 60 min. After washing with PBS, tissue sections were incubated in secondary antibodies (LI-COR, USA) at 37 °C for 60 min. We used the DAB substrate system to develop the color. The images were captured in a bright field digital microscope and the analysis was performed by open source Image J software (NIH, USA).

2.6. qPCR

Total RNA was extracted from the tissue using the MiniBEST Universal RNA Extraction kit (Takara, Japan). Then cDNA was prepared using RNA reverse transcription kit PrimeScript™ RT reagent (Takara, Japan). The gene expression was analyzed by using qPCR kit SYBR Premix Ex Taq II (Takara, Japan). The relative quantitative analysis of gene expression has complied with the $2^{-\Delta\Delta\text{ct}}$ method. All specific primer sequences used in experiments were listed in Table 2.

Table 2
List of specific primer sequences

Sl.no	Gene name	Primer	Rat sequence 5'-3'	Human sequence 5'-3'
1	AQP1	AQP1-F	CTGGATGTGGTTGCTGTGGT	CCGCAATGACCTGGCTGATGG
		AQP1-R	CCTCCATGTAGCAGGCATTG	CGCCTCCGGTCGGTAGTAGC
2	β -actin	β -actin-F	GCTCTCTTCCAGCCTTCCTT	GGGACCTGACTGACTACCTC
		β -actin-R	GGTCTTTACGGATGTCAACG	TCATACTCCTGCTTGCTGAT

2.7. Western blot

Total protein was extracted from the renal tissue in RIPA lysis buffer (Beyotime, China) mixed with 1% phosphatase inhibitor (CW BIO, China), 1% protease inhibitor (CW BIO, China) and 1% PMSF (Beyotime, China). The protein concentration was estimated by BCA method. The protein was separated in SDS-PAGE gel and then transferred onto a PVDF membrane (162–0177, BIO-RAD, USA). The membranes were blocked in 5% skimmed milk (BD, America) in PBST for 90 min, and later, were incubated in primary antibodies (anti-Aquaporin 1 (Abcam, UK), anti-CD34 (HUABIO, China), anti-VEGF (HUABIO, China), anti- β -actin (HUABIO, China)) for overnight at 4 °C. Later, the primary antibody labeled membranes were incubated with specific secondary antibodies. The protein expression was visualized through Odyssey two-color infrared laser imaging system (Odyssey Clx, USA), and was analyzed with the formula:

$$\text{Relative gray value} = \left(\frac{\text{sample gray value} / \text{sample internal parameter}}{\text{control gray value} / \text{control internal parameter}} \right)$$

2.8. SQW containing serum isolation and purification

Twenty SPF male SD rats were marked and weighed, and randomly divided into two groups: normal control group and SQW (3.0 g / kg) group, with 10 rats in each group. The rats in SQW group were given gavage of 100 g / 1 mL by intragastric administration twice a day for 5 consecutive days. The normal control group was given the same volume of saline. During the administration period, the rats were on a normal diet. They were not provided with food but water was allowed 12 hours before the last administration.

After the last dose of SQW administration, rats were anesthetized and cardiac blood was collected under aseptic condition. The cardiac blood of the rats was allowed to stand for 1 h after isolation and centrifuged at 3,000 rpm for 15 min to obtain the rat serum. The collected serum was sterilized by filtration 0.22 μm filter (Millipore, USA). The sterilized serum was then heat-inactivated at 56 °C for 30 min in a water bath.

2.9. Cell culture

HMEC-1 cells (iCell Bioscience, China) were grown in Endothelial Cell Medium (ECM) containing 10% fetal bovine serum (FBS), 10 ng/ml Epidermal Growth Factor (EGF), 1 $\mu\text{g}/\text{ml}$ hydrocortisone acetate, 10 mM glutamine, 1% penicillin and streptomycin (1:1). The cells were maintained in an incubator with 5% carbon dioxide (Thermo, USA) at 37 °C temperature. The cells were administrated with different doses of serum containing SQW and normal serum. The specific groups are as follows: 10% of normal rat serum containing group (10% NRS), 5% each of SQW-normal rat serum mix group (5% SQW + 5% NRS), and different concentrations of SQW-containing serum were diluted with normal rat serum. The cells were starved for 2 h in a serum-free medium before the treatment.

2.10. AQP1 RNAi Lentivirus transduction

2×10^5 HMEC-1 cells were seeded in a 6-well plate and incubated for 24 hours and transduced with RNAi-expressing lentivirus particles. The RNAi-AQP1 lentivirus (V1 and V2) and negative control lentivirus (NC) were purchased from Genechem Co., LTD (Shanghai, China). AQP1 transfection efficiency was observed after three days from the transduction by fluorescence microscopy, qRT-PCR and Western Blot.

2.11. Cell scratch assay (migration assay)

3×10^5 HMEC-1 cell was seeded in a 6-well plate. Before the treatment, the cells were washed with PBS (Solarbio, China), and each group was added with corresponding drug-containing serum and

photographed at 0 h, 6 h, 12 h, 24 h. Analysis of the migration area was determined by LAS V4.4 software.

2.12. In vitro lumen formation assay

60 μ L/well Matrigel gel was added to the 96-well plate and placed in the incubator for 30 minutes to solidify. The HMEC-1 cell suspension was prepared and added to the 96-well plate containing Matrigel gel. Then different types of serum, VEGF (8 ng/ml; positive control group) were added. After culturing for 4 h at 37 °C incubator, random fields were selected and photographed. The image was processed by Image J software.

2.13. Statistical analysis

The SPSS19.0 statistical software was used to perform a normality test on each set of data, which was confirmed to the normal distribution, using One-Way ANOVA. If the equation is homogeneous, the LSD test was used. If the equation was not uniform, we used Games-Howell (A) test; $p < 0.05$ and $p < 0.01$ were considered as statistically significant.

Results

3.1. Effect of SQW on renal morphological

The renal injury was induced by adenine treatment in the rat. Here, we examined whether SQW was able to ameliorate the toxicity and injury caused by adenine. To find out the morphological damage, we performed H&E staining to understand the structure and integrity of the kidney. As is shown in Fig. 1.A of H&E staining, the adenine treated rats were containing renal injury as the structure and morphology of glomeruli and renal tubules were deformed and damaged. More specifically histological examination revealed that in the adenine treated (model) group, the glomerulus internal structures were collapsed, the renal tubules dilated, the lumens deposited, and the renal tubules blocked while compared with control groups. After the administration of different doses of SQW, the adenine mediated structural damages were reformed in renal injury. More specifically, the collapsed parts of glomerulus were reduced, the renal tubule structure was reformed, the capsule was tightly bound, and the renal pathology of the rat was improved. Therefore, we found that the SQW was able to protect the renal tissue from adenine mediated damages.

3.2. Biochemical analysis of renal toxicity

Renal toxicity caused by adenine in the rat model was observed and that can cause structural damages in the kidney. Therefore, to observe the pathological deformities, we examined different serum pathological markers, namely, BUN, Scr, U-TP and Ccr. These markers pointed out the severity of the pathogenesis and level of kidney activity. As is shown in Fig. 1.B-E, we used the level of BUN, Scr, U-TP/24 h, and Ccr to manifest renal function of rats. The level of BUN ($P < 0.01$), Scr ($P < 0.01$) and U-TP/24 h ($P < 0.01$) were significantly elevated in the model group while comparing with the normal control

groups and in contrast, Ccr ($P < 0.01$) level was decreased in the model group as compared with the normal control group. Next, we examined the potential of SQW therapy on the adenine treated model rats. The corresponding indicators' changes pointed out the beneficiary nature of the drug in reducing the renal toxicity. We found that the indicators were all reversed after SQW treatment, suggesting SQW could protect kidney injury in adenine induced rats.

3.3. HPA axis functioning analysis

Next we examined different enzymatic markers' level hypothalamic corticotrophin-releasing factor (CRH), adrenocorticotrophic hormone (ACTH), cortisol (CORT) and urinary 17-hydroxy corticosteroid (17-OHCS) by ELISA assay. Adenine treatment in the rat observed in Fig. 2.A-D was toxic as the CRH ($P < 0.01$), ACTH ($P < 0.01$), CORT ($P < 0.01$) and 17-OHCS ($P < 0.01$) level was diminished compared with normal control rats. Moreover, treatment with SQW has elevated the enzyme level in rats, indicating the reduction of toxicity in the SQW treated rat groups.

3.4. Recovery of VEGF expression by SQW in renal tissues

To examine the effect of SQW on alleviating perivascular capillary damage induced by adenine in rats, we immune-stained the tissue with anti-VEGF antibodies in rat kidney sections. It is known that decreased VEGF expression level of kidney tissue reflects the severity of perivascular capillary loss by infection or toxicity. As shown in Fig. 3.A, the stained tissue sections indicated that the VEGF expression was mainly observed on the cell membrane and cytoplasm regions. The adenine treated rats' kidney histological sections indicated the reduction in VEGF expression while comparing with normal control groups. Moreover, the capillary damages were observed in these groups as the cell density was also reduced. On the other hand, 3 g/kg SQW obviously enhanced VEGF expression compared with model group.

3.5. Recovery of perivascular capillary density by SQW in renal tissue

Perivascular capillary density was labeled by anti-CD34 antibody staining. We found that the CD34 staining was reduced in the model group of rats while comparing with the control group. Therefore, the perivascular capillary loss was prominent in the adenine treated group. So to examine the recovery of perivascular capillary loss by SQW treatment, we quantified our observation of CD34 staining. We observed the dose of 3 g/kg SQW was most effective against adenine toxicity (Fig. 3.B).

3.6. Ameliorating inflammatory cytokines by SQW in renal tissue

To evaluate vascular inflammation, circulating levels of VCAM-1, and MCP-1 levels were examined, as they are related to inflammatory injury of capillary endothelial cells, inducing capillary dropout. As is shown in Fig. 3.C-D, VCAM-1 ($P < 0.01$) and MCP-1 ($P < 0.01$) expression was increased in the model group compared with the normal control group. VCAM-1 and MCP-1 expression was reduced in SQW groups

versus model group. These findings supported that the protective role of SQW in perivascular capillary injury (Fig. 3.C-D).

3.7. Effect of SQW on AQP1 in kidney

AQP1 abundantly expresses in the nephron and mostly regulates the osmotic balance in the kidney cells. Moreover, AQP1 regulates the proliferation of perivascular capillary. Therefore, we examined and quantitated the expression pattern of AQP1 in mRNA and protein level by qPCR and Western blot method, respectively. We observed the adenine treatment significantly suppressed the AQP1 expression in both mRNA and protein levels. Moreover, we ameliorated the AQP1 expression level in the groups that were supplemented with SQW. In our next set of experiments, we stained the kidney tissue with the AQP1 antibody to understand the expression pattern and localization in the kidney tissue. We found that the AQP1 was robustly expressed in the perivascular capillary region. Damages in the kidney by adenine reduces AQP1 expression at the perivascular capillary thus indicating the importance of AQP1 in maintaining the homeostasis of the kidney. Our treatment protocol with different doses of SQW potentially ameliorated the damages by reforming the structure of the perivascular capillary region and also enhanced the expression level of AQP1 (Fig. 4.C). Thus we speculated that SQW was beneficial to protect the kidney cells by maintaining AQP1 expression possibly.

3.8. Effect of SQW medicated serum on cell migration and lumen forming capacity

To verify our speculation, we adopted a lentivirus-mediated knockdown system to knockdown AQP1 on the HMEC-1 cell line. The findings indicated that the lentiviral-mediated AQP1 RNAi could efficiently and stably weaken the AQP1 level in HMEC-1 cells, and knockdown efficiency of the lentivirus V2 group is especially remarkable that chosen for further study (Fig. 5.A-B).

According to the above result, 3 g/kg SQW was the most efficient dose to protect perivascular capillary damage, thus we chose that to prepare SQW medicated serum for following cell experiment. We found in Fig. 5C that SQW upregulated AQP1 protein level compared with control group (NC-10%NRS) and also inhibited downregulated AQP1 protein level with AQP1 knockdown (V2-10%NRS). Moreover, AQP1 knockdown markedly reduced scratch healing rate and lumen formation ability versus NC (Negative control)-10%NRS group, accordingly, the ability of cell migration and lumen formation were attenuated by SQW medicated serum (Fig. 6A-B).

Discussion

CKD accompanied by a silent loss of function of the kidney due to different disorders like diabetes, high blood pressure, glomerulonephritis, interstitial nephritis, polycystic kidney disease. CKD is an undecorated public health problem. A large number of the population is affected by CKD. In this article, we describe the effect of SQW on an animal model of CKD. The beneficial effect of SQW is clearly described in this article

and we delineated the working principle of SQW on CKD disorder in cell lines and animal models. There is a probability to withstand with the CKD is to targeted repair of peritubular capillary endothelium. The improvement of disease management could be achieved by understanding the relation between endothelium and CKD. The adopted therapy in this study was able to ameliorate the tissue damage caused by adenine. Moreover, we examined the relationship of angiogenesis in endothelial cells.

The animal model provides a meaningful platform to examine the underlying mechanism of therapy against CKD. The adenine-induced rat model is one of the successfully-adopted CKD models, manifested in the appearance of the corresponding symptom of CKD, such as lesions of proximal tubules, of some distal tubules and glomeruli (22). In this study, we relied on a well-established kidney injury animal model and examined the protective effect of SQW. Adenine treatment-induced destruction of renal structure and function in rats' renal tissue appeared. The pathological markers- BUN, Scr and U-Pro/24 h, morphological changes of kidney fibrosis were according to the conventional CKD syndrome (12). Serum BUN, SCr and U-Pro/24 h urine protein are the indicators of renal function, we found a significant increase of those proteins in CKD. Moreover, with SQW a reduced serum BUN, SCr and 24-h urine protein were observed, indicating an improvement in renal function. Hypothalamic-pituitary-adrenal (HPA) axis markers including CRH, ACTH, CORT, and 17-OHCS are associated with end-stage renal disease, which is highly suppressed in CKD patients (23). The hormonal imbalance was observed in CKD disorder. Adenine administration was caused an increase in these hormonal levels. Our model therapy system was shown improvement.

Consequently, peritubular capillary injury in kidney tissue with adenine was noticed, is usually accompanied with CKD (24), subsequent loss of peritubular capillaries is a common feature of progressive renal disease (25), which is common in both animal models and patients of renal disease. At this stage, the function of the endothelial cells uses to compromise (26). Endothelial cells, serving as the inner lining of the vessel wall, often assemble to form a lumen and consist of many blood vessels that served to supply and delivery of nutrients and oxygen in the body(27, 28). The endothelium cells are the main components of blood vessels, and thus, playing a nodal role in angiogenesis. Previous pieces of evidence showed that VEGF plays a key mediator of vascular formation (29). Physiological events including cell proliferation, migration, survival, and vascular permeability during vasculogenesis and angiogenesis were affected by VEGF signaling through regulating the activities of several kinases (30). The result of our research indicated that the group related to peritubular injury was shown a low level of VEGF expression and as per the earlier findings (31).

Water channel protein-AQP1 maintains the osmotic balance in the renal cells and associates with cell migration and angiogenesis (32). Recently adequate evidence supported that inhibition of AQP1 relates to impaired migration, invasion and tubulogenesis in vitro (33). We have shown AQP1 knockdown inhibited cell migration and tube formation that was enhanced by SQW administration. Moreover, SQW was able to upregulate AQP1 expression in the cells in vitro and in vivo. The establishment of a novel pathway for SQW was determined in this study, as, we uncover the AQP1 was responsible for the ameliorating effect for SQW in the renal tissues. The silencing of AQP1 diluted the effect of SQW in the in vitro conditions. Future studies would be needed to fully prove the findings in the in vivo knockout

system. But the preliminary data was encouraging, which delineated the molecular pathway for SQW in CKD pathogenesis in vitro and in vivo.

In conclusion, SQW could act as a remedy for peritubular capillary injury in adenine-induced CKD rats, meanwhile, SQW treatment enhanced AQP1 expression in the renal cells and tissues. We studied SQW on the angiogenesis process, and the process was hampered in the CKD model system. It was turned out that SQW administration attenuates renal vascular injury through boosting the angiogenesis of endothelial cells. The protective effect of SQW on the angiogenesis of endothelial cells provided a novel perspective for the treatment of CKD.

Conclusion

In our study, SQW could alleviate and was associated peritubular capillary injury in adenine-induced CKD rats with the increase of AQP1 mRNA and protein expression levels, suggesting that SQW could act as a remedy for renal injury. Therefore, AQP1 may be a potential target of SQW for treating renal injury.

List Of Abbreviations

SQW	Shen-Qi-Wan
CKD	Chronic kidney disease
TCM	Traditional Chinese Medicine
HPA	Hypothalamic-Pituitary-Adrenal
BUN	blood urea nitrogen
Scr	serum creatinine
U-TP	urine protein excretion
Ccr	creatinine clearance
VEGF	vascular endothelial growth factor
VCAM-1	vascular cell adhesion molecule-1
MCP-1	monocyte chemotactic protein-1
AQP1	Aquaporin-1
CRH	hypothalamic corticotrophin-releasing factor
ACTH	adrenocorticotrophic hormone

CORT	cortisol
17-OHCS	urinary 17-hydroxy corticosteroid
HMEC-1	Human Microvascular Endothelial Cell line-1
NRS	normal rat serum
ECs	endothelial cells.

Declarations

Acknowledgments

We are indebted to the members of our laboratories at the Department of pharmacology, University of Zhejiang Chinese Medical.

Authors' contribution

YTB and YHZ contributed equally to this work. YTB, LTJ and CYL designed the experiments. YTB, XMC, LNL and YBF performed the experiments. YHZ analyzed data. YXY, LTJ and CYL supervised the project. YHZ wrote the paper.

Consent to publish

This manuscript is approved by all authors for publication.

Declaration of conflicting interests

The author(s) declared no potential conflicts of interest with respect to the research, authorship, and/or publication of this article.

Funding

This work is supported by National Natural Science Foundation of China (Grant No.8167151544).

Ethics approval and consent to participate

The animal experiments were approved by the Animal Care and Use Committee of Zhejiang Chinese medical university (Approval Number: ZSLL-2014-59).

Availability of data and materials

All data of this study can be found within the manuscript and available from the corresponding author upon request.

Competing interests

The authors declare that they have no competing interests.

Footnotes

Publisher's Note

Springer Nature remains neutral with regard to jurisdictional claims in published maps and institutional affiliations.

Yuting Bao and Yehui Zhang contributed equally to this study.

References

1. Romagnani P, Remuzzi G, Glasscock R, Levin A, Jager KJ, Tonelli M, et al. Chronic kidney disease. *Nat Rev Dis Primers*. 2017;3:17088.
2. Wuttke M, Li Y, Li M, Sieber KB, Feitosa MF, Gorski M, et al. A catalog of genetic loci associated with kidney function from analyses of a million individuals. *Nat Genet*. 2019;51(6):957-72.
3. Qiu C, Huang S, Park J, Park Y, Ko YA, Seacock MJ, et al. Renal compartment-specific genetic variation analyses identify new pathways in chronic kidney disease. *Nat Med*. 2018;24(11):1721-31.
4. Munoz-Felix JM, Oujo B, Lopez-Novoa JM. The role of endoglin in kidney fibrosis. *Expert Rev Mol Med*. 2014;16:e18.
5. Schainuck LI, Striker GE, Cutler RE, Benditt EP. Structural-functional correlations in renal disease. II. The correlations. *Hum Pathol*. 1970;1(4):631-41.
6. Li L, Kang H, Zhang Q, D'Agati VD, Al-Awqati Q, Lin F. FoxO3 activation in hypoxic tubules prevents chronic kidney disease. *Journal of Clinical Investigation*. 2019;129(6):2374-89.
7. Babickova J, Klinkhammer BM, Buhl EM, Djurdjaj S, Hoss M, Heymann F, et al. Regardless of etiology, progressive renal disease causes ultrastructural and functional alterations of peritubular capillaries. *Kidney Int*. 2017;91(1):70-85.
8. Rabelink TJ, Wijewickrama DC, de Koning EJ. Peritubular endothelium: the Achilles heel of the kidney? *Kidney Int*. 2007;72(8):926-30.
9. Venkatachalam MA, Weinberg JM, Kriz W, Bidani AK. Failed Tubule Recovery, AKI-CKD Transition, and Kidney Disease Progression. *J Am Soc Nephrol*. 2015;26(8):1765-76.
10. Eelen G, de Zeeuw P, Treps L, Harjes U, Wong BW, Carmeliet P. Endothelial Cell Metabolism. *Physiol Rev*. 2018;98(1):3-58.
11. Wang X, Zhang A, Zhou X, Liu Q, Nan Y, Guan Y, et al. An integrated chinmedomics strategy for discovery of effective constituents from traditional herbal medicine. *Sci Rep*. 2016;6:18997.
12. Chen H, Xu Y, Yang Y, Zhou X, Dai S, Li C. Shenqiwan Ameliorates Renal Fibrosis in Rats by Inhibiting TGF-beta1/Smads Signaling Pathway. *Evid Based Complement Alternat Med*. 2017;2017:7187038.

13. Yen ML, Su JL, Chien CL, Tseng KW, Yang CY, Chen WF, et al. Diosgenin induces hypoxia-inducible factor-1 activation and angiogenesis through estrogen receptor-related phosphatidylinositol 3-kinase/Akt and p38 mitogen-activated protein kinase pathways in osteoblasts. *Mol Pharmacol*. 2005;68(4):1061-73.
14. Dong W, Xian Y, Yuan W, Huifeng Z, Tao W, Zhiqiang L, et al. Catalpol stimulates VEGF production via the JAK2/STAT3 pathway to improve angiogenesis in rats' stroke model. *J Ethnopharmacol*. 2016;191:169-79.
15. Verkman AS, Anderson MO, Papadopoulos MC. Aquaporins: important but elusive drug targets. *Nat Rev Drug Discov*. 2014;13(4):259-77.
16. van Koppen A, Joles JA, Bongartz LG, van den Brandt J, Reichardt HM, Goldschmeding R, et al. Healthy bone marrow cells reduce progression of kidney failure better than CKD bone marrow cells in rats with established chronic kidney disease. *Cell Transplant*. 2012;21(10):2299-312.
17. Zhang Y, Nakano D, Guan Y, Hitomi H, Uemura A, Masaki T, et al. A sodium-glucose cotransporter 2 inhibitor attenuates renal capillary injury and fibrosis by a vascular endothelial growth factor-dependent pathway after renal injury in mice. *Kidney Int*. 2018;94(3):524-35.
18. Palethorpe HM, Tomita Y, Smith E, Pei JV, Townsend AR, Price TJ, et al. The Aquaporin 1 Inhibitor Bacopaside II Reduces Endothelial Cell Migration and Tubulogenesis and Induces Apoptosis. *Int J Mol Sci*. 2018;19(3).
19. Zhou F, Qian Z, Huang L. Low-dose mifepristone increased angiogenesis in a manner involving AQP1. *Arch Gynecol Obstet*. 2019;299(2):579-84.
20. A-xu Z. Determination of Morroniside, Loganin and Paeonol in Guifu Dihuang Pills (Concentrated Pills) by HPLC. *Strait Pharmaceutical Journal*. 2018;30(10):66-68. *Strait Pharmaceutical Journal*. 2018;30(10):66-8.
21. Zhang JY, Hong CL, Chen HS, Zhou XJ, Zhang YJ, Efferth T, et al. Target Identification of Active Constituents of Shen Qi Wan to Treat Kidney Yang Deficiency Using Computational Target Fishing and Network Pharmacology. *Front Pharmacol*. 2019;10:650.
22. Yokozawa T, Zheng PD, Oura H, Koizumi F. Animal model of adenine-induced chronic renal failure in rats. *Nephron*. 1986;44(3):230-4.
23. Cardoso EM, Arregger AL, Budd D, Zucchini AE, Contreras LN. Dynamics of salivary cortisol in chronic kidney disease patients at stages 1 through 4. *Clin Endocrinol (Oxf)*. 2016;85(2):313-9.
24. Kramann R, Tanaka M, Humphreys BD. Fluorescence microangiography for quantitative assessment of peritubular capillary changes after AKI in mice. *J Am Soc Nephrol*. 2014;25(9):1924-31.
25. Tanaka T, Nangaku M. Angiogenesis and hypoxia in the kidney. *Nat Rev Nephrol*. 2013;9(4):211-22.
26. Ligresti G, Nagao RJ, Xue J, Choi YJ, Xu J, Ren S, et al. A Novel Three-Dimensional Human Peritubular Microvascular System. *J Am Soc Nephrol*. 2016;27(8):2370-81.
27. Rohlenova K, Veys K, Miranda-Santos I, De Bock K, Carmeliet P. Endothelial Cell Metabolism in Health and Disease. *Trends Cell Biol*. 2018;28(3):224-36.

28. Watson EC, Grant ZL, Coultas L. Endothelial cell apoptosis in angiogenesis and vessel regression. *Cell Mol Life Sci.* 2017;74(24):4387-403.
29. Carmeliet P, Ferreira V, Breier G. Abnormal blood vessel development and lethality in embryos lacking a single VEGF allele. *Nature.* 1996;380:435-9.
30. Apte RS, Chen DS, Ferrara N. VEGF in Signaling and Disease: Beyond Discovery and Development. *Cell.* 2019;176(6):1248-64.
31. Krieter DH, Fischer R, Merget K, Lemke HD, Morgenroth A, Canaud B, et al. Endothelial progenitor cells in patients on extracorporeal maintenance dialysis therapy. *Nephrol Dial Transplant.* 2010;25(12):4023-31.
32. Narvaez-Moreno B, Sendin-Martin M, Jimenez-Thomas G, Sanchez-Silva R, Suarez-Luna N, Echevarria M, et al. Expression patterns of aquaporin 1 in vascular tumours. *Eur J Dermatol.* 2019;29(4):366-70.
33. Shu C, Shu Y, Gao Y, Chi H, Han J. Inhibitory effect of AQP1 silencing on adhesion and angiogenesis in ectopic endometrial cells of mice with endometriosis through activating the Wnt signaling pathway. *Cell Cycle.* 2019;18(17):2026-39.

Figures

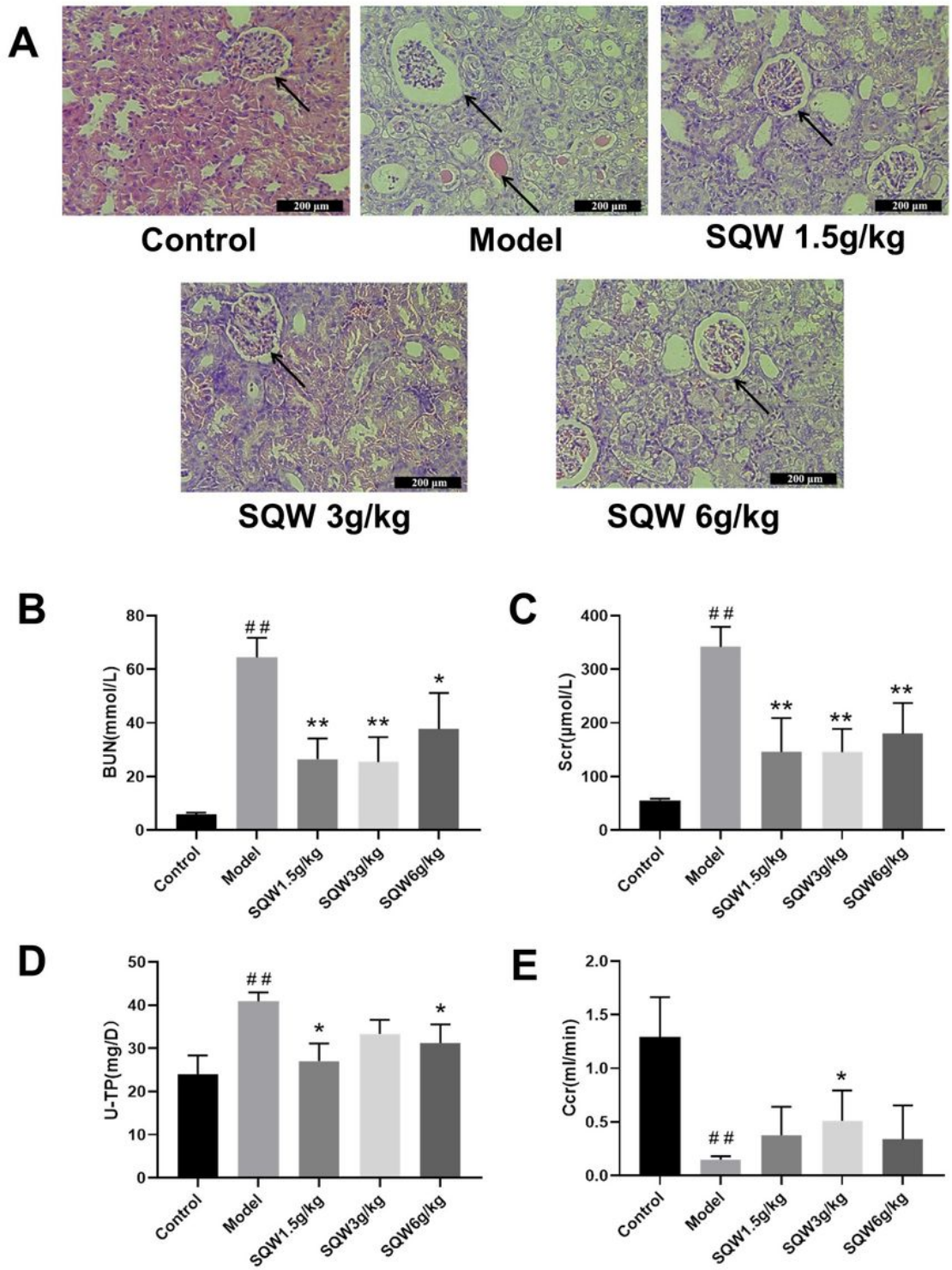


Figure 1

The effect of SQW on kidney injury in rats. (A) Respective images of HE stained kidney tissue. (B-E) Indices for renal function, including levels of blood urea nitrogen (BUN), serum creatinine (Scr), 24-hour urine protein excretion (U-TP) and creatinine clearance (Ccr) in rats. n=6. Small horizontal bars indicate the mean±s.d. # P<0.05, ## P<0.01 compared with control group; * P<0.05, ** P<0.01 compared with model group.

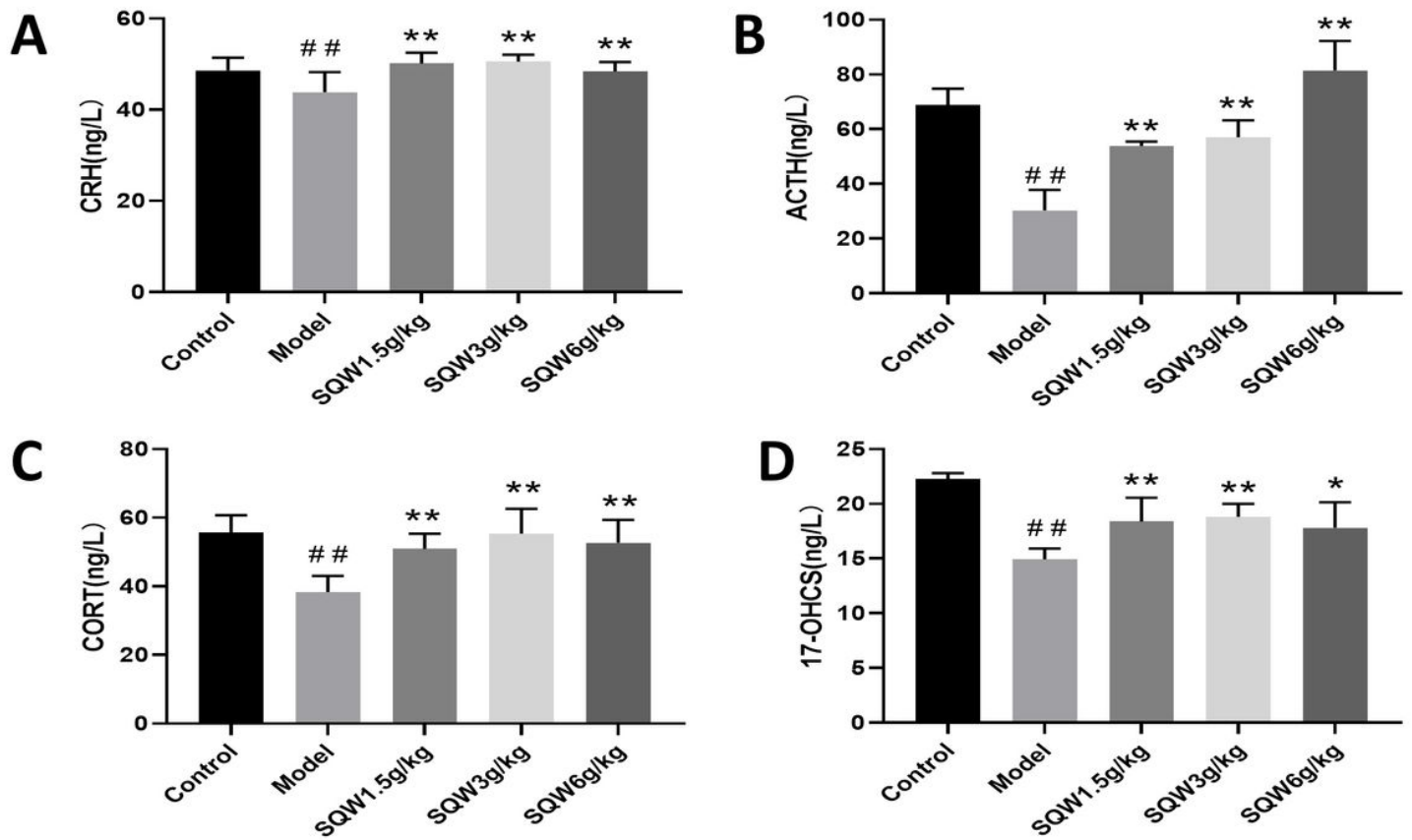


Figure 2

The effect of SQW on CRH, ACTH, CORT and 17-OHCS in rats. (A-D) Indices for well-established CKD model rats, including levels of hypothalamic CRH, serum ACTH, CORT and urine 17-OHCS in rats. n=6. Small horizontal bars indicate the mean ± s.d. # P < 0.05, ## P < 0.01 compared with control group; * P < 0.05, ** P < 0.01 compared with model group.

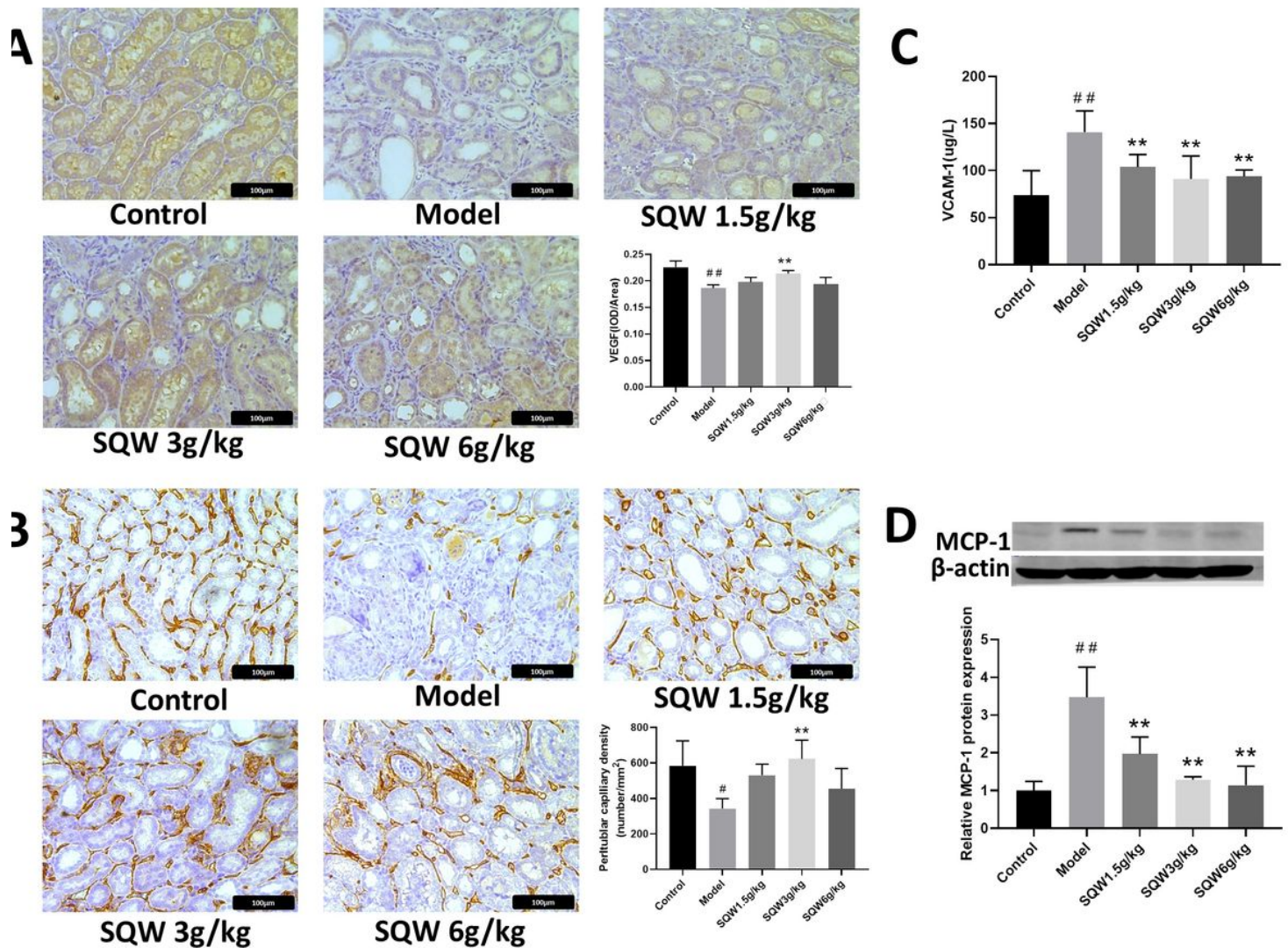


Figure 3

The effect of SQW on capillary endothelium of renal tubule in rats. (A) Indices for perivascular capillary damage- Immunohistochemistry was allowed to assess the vascular endothelial growth factor (VEGF) in kidney tissue of rats. Brown granules are positive expression of VEGF protein. n=3. (B) Indices for perivascular capillary injury- Immunohistochemistry of CD34 protein in the kidney of rats. CD34 protein is localized in the cell membrane. Brown or tan granules were positive CD34 protein. n=3. (C) Indices for inflammation followed by perivascular capillary injury-The serum level of pro-inflammatory cytokine vascular cell adhesion molecule-1 (VCAM-1) in rats. n=6. (D) Indices for inflammation followed by perivascular capillary injury-Western blot of monocyte chemotactic protein-1 (MCP-1) in kidney tissue of rats. n=6. Small horizontal bars indicate the mean±s.d. # P<0.05, ## P<0.01 compared with control group; * P<0.05, ** P<0.01 compared with model group.

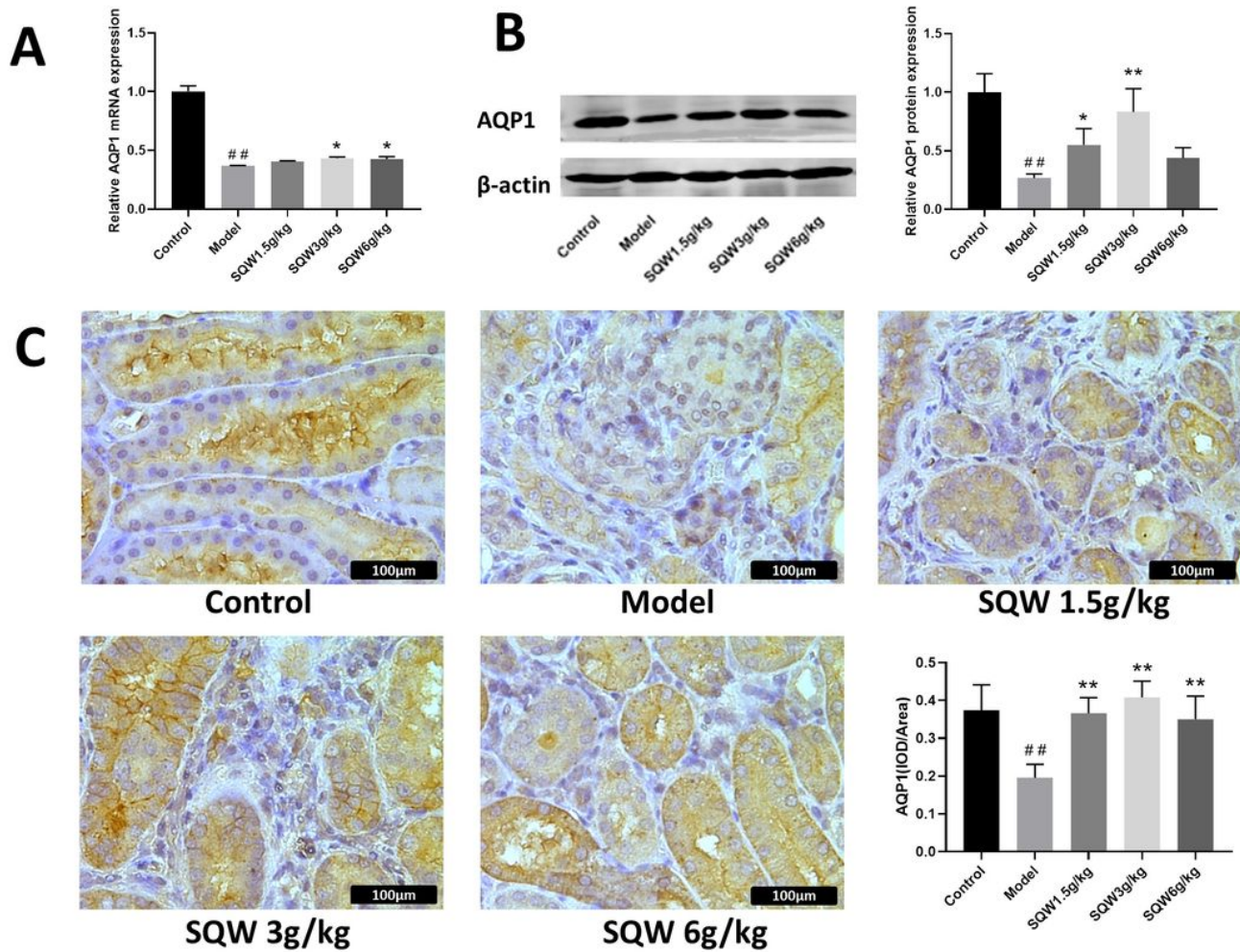


Figure 4

The effect of SQW on renal AQP1 expression level. (A) The AQP1 mRNA level in the kidney of SD rats was measured by qPCR. n=6. (B) Analysis of AQP1 protein in the kidney of SD rats through Western blot. n=6. (C) Evaluations of AQP1 expression in the kidney of SD rats through immunohistochemistry. n=3. AQP1 is mainly expressed in cytoplasm and cell membrane. Brown granules were positive AQP1 protein. Small horizontal bars indicate the mean±s.d. # P<0.05, ## P<0.01 compared with control group; * P<0.05, ** P<0.01 compared with model group.

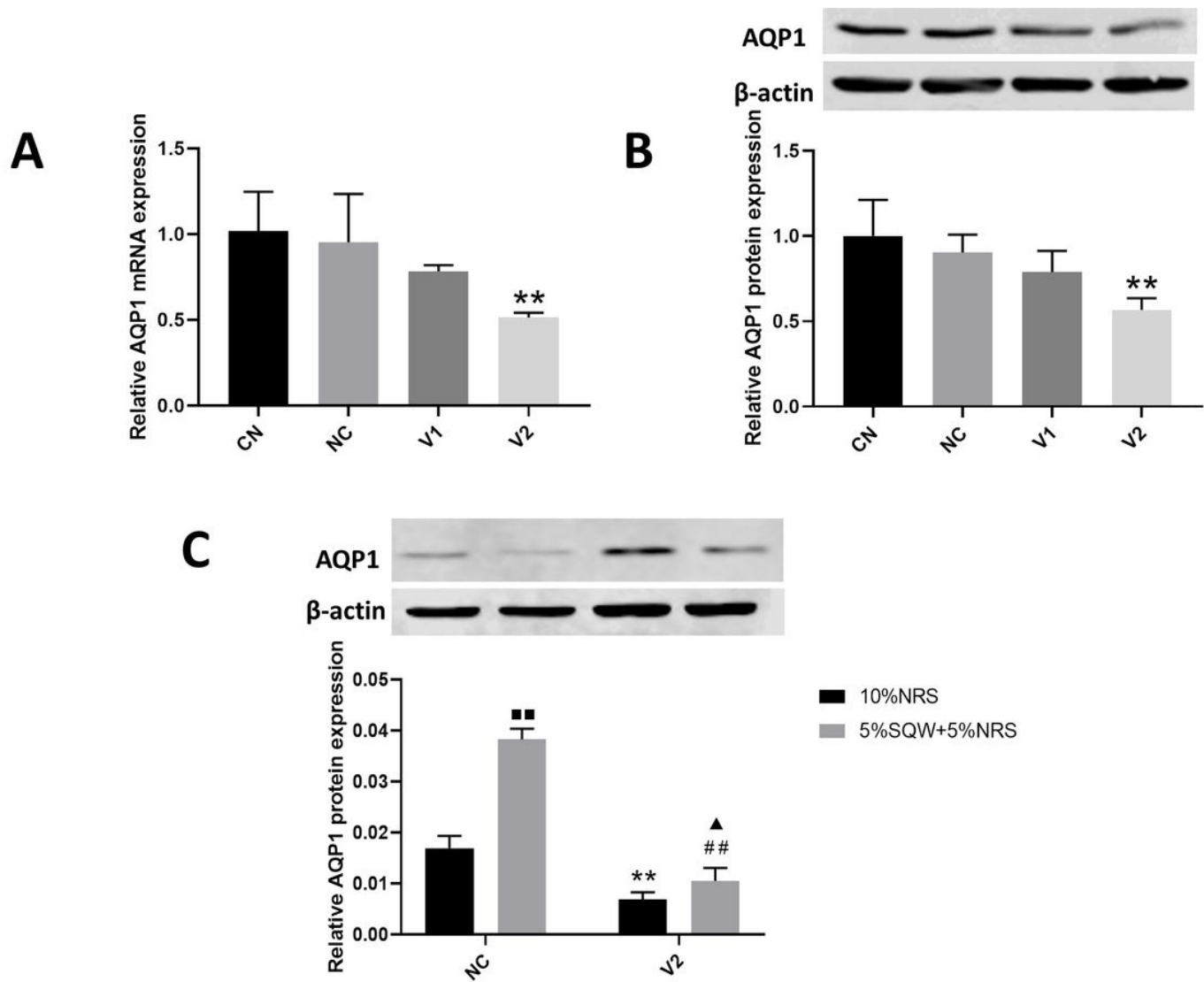


Figure 5

Effect of AQP1 knockdown on the AQP1 expression in HMEC-1 Cells. (A) Effect of different interference targets of AQP1 RNAi lentivirus (V1, V2) and negative control (NC) on mRNA expression of AQP1 in HMEC-1 cells. n=4, mean \pm s.d. ** P<0.01 compared with negative control group. (B) Effect of different interference targets of AQP1 RNAi lentivirus (V1, V2) and negative control (NC) on protein expression of AQP1 in HMEC-1 cells. n=4, mean \pm s.d. ** P<0.01 compared with negative control group. (C) With lentivirus V2 and SQW (3 g/kg) medicated serum treatment, the protein expression of AQP1 was detected by western blot. n=4, mean \pm s.d. ■ P<0.05, ■ ■ P<0.01 compared with NC-10%NRS; # P<0.05, # # P<0.01 compared with V2-10% NRS; ** P<0.01 compared with NC-10%NRS; ▲ P<0.05 compared with NC-5% SQW+5% NRS. (CN: control group, NC: negative control group, V1: the lentivirus V1 group, V2: the lentivirus V2 group, NRS: Normal rat serum)

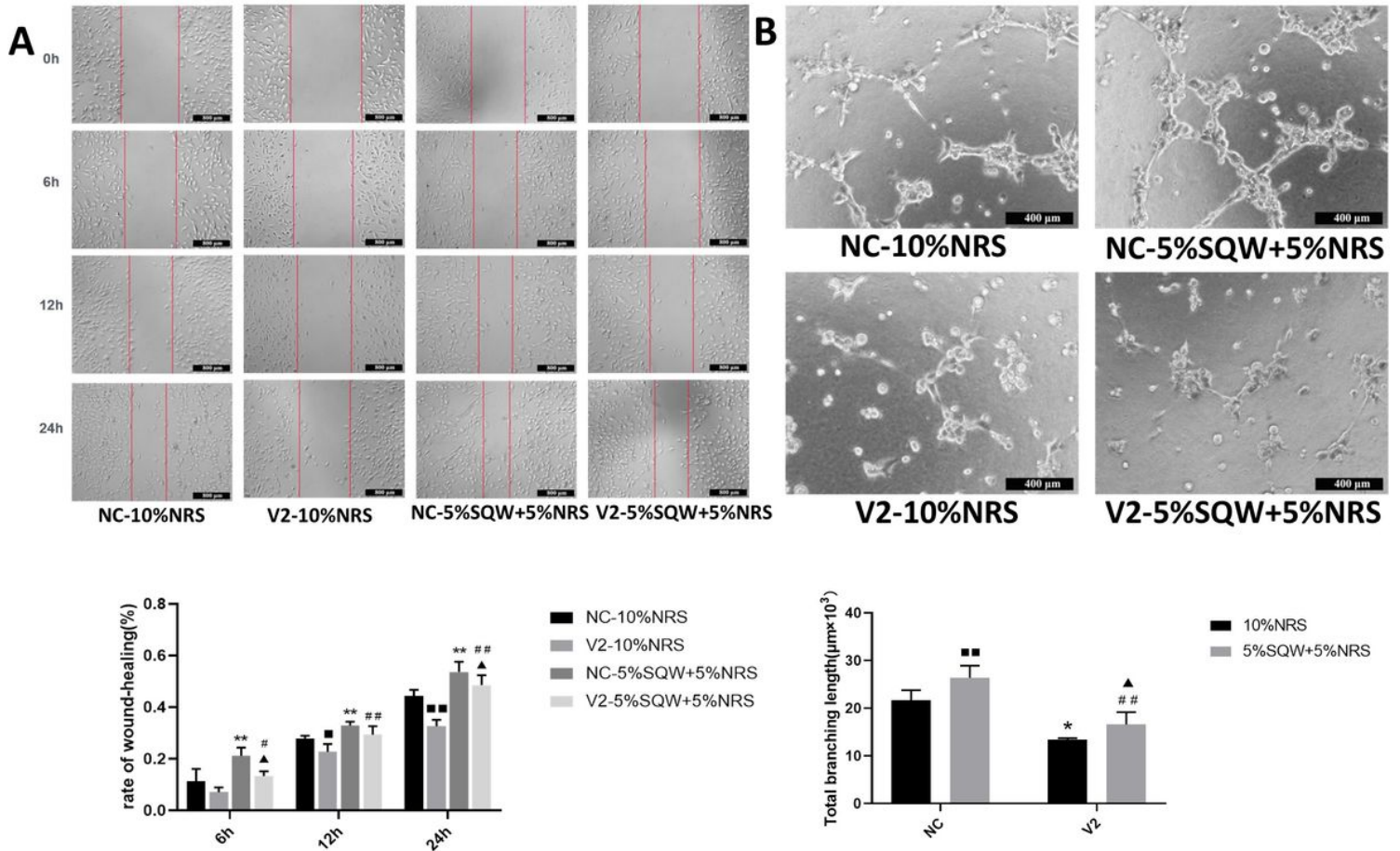


Figure 6

Effect of SQW on promoting cell migration and tube formation after AQP1 knockdown in HMEC-1 Cells. (A) Indices for angioplasty ability-Representative images of cell migration. $n=4$, mean \pm s.d. ■■P<0.01 compared with NC-10%NRS, **P<0.01 compared with NC-10%NRS, ▲P<0.05 compared with V2-10% NRS, ## P<0.01 compared with NC-5% SQW+5% NRS. (B) Indices for angioplasty ability-Representative images of tube formation. $n=4$, mean \pm s.d. ■■P<0.01 compared with NC-10%NRS, *P<0.01 compared with NC-10%NRS, ▲P<0.05 compared with V2-10% NRS, ## P<0.01 compared with NC-5% SQW+5% NRS.